

Available online at www.sciencedirect.com

ScienceDirect

journal homepage: <http://www.elsevier.com/locate/acme>

Original Research Article

Imperfection sensitivity analysis of steel columns at ultimate limit state

Zdeněk Kala^{*}, Jan Valeš

Brno University of Technology, Faculty of Civil Engineering, Department of Structural Mechanics, Veveri Street 95, 602 00 Brno, Czech Republic

ARTICLE INFO

Article history:

Received 1 September 2017

Accepted 13 January 2018

Available online

Keywords:

Sobol sensitivity analysis

Steel structure

Buckling

Imperfections

Finite element

ABSTRACT

The present paper applies Sobol's variance-based global sensitivity analysis (SSA) to quantify the contribution of input imperfections to the load-carrying capacity (LCC) of an IPN 200 steel compressed member. LCC is evaluated using the geometrically and materially non-linear finite element solution with regard to the effects of initial random imperfections including residual stresses. Comparison of results of SSA for (i) buckling about the minor principal axis, (ii) buckling about the major principal axis and (iii) lateral-torsional buckling due to bending moment is performed on the non-dimensional slenderness interval of 0–2. SSA for (i) and (ii) is performed for steel grade (a) S235 and (b) S355, SSA for (iii) is performed only for steel grade S235. SSA found similarities in results (ia) and (ib), (iia) and (iib) and identified significant differences between results (ia) and (iia), (iia) and (iiaa), where sensitivity to the initial axial curvature is more than two times higher in (ia) than in (iiaa). The relationships between the effects of initial imperfections on LCC and the design criteria of reliability of Eurocode 3 are discussed.

© 2018 Politechnika Wroclawska. Published by Elsevier Sp. z o.o. All rights reserved.

1. Introduction

Initial geometric and material imperfections including residual stresses influence the reliability of load bearing steel members, which are subjected to compression or strong axial bending and compression associated with other action effects [1]. In probabilistic modelling, initial imperfections are treated as random variables, see e.g. [2,3]. The basis of probabilistic modelling is the stochastic computational model, whose inputs are random imperfections and output is a random variable, which is crucial for the assessment of adverse phenomena [4,5].

Adverse effects inherent in structural design are usually associated with the attainment of any of the limit states [6,7] established in standards [8,9], during which the structure or a part of the structure no longer satisfies requirements, see e.g. [10–12]. Probabilistic structural design is a decision problem [13,14] added to probabilistic structural analysis [15], in which the probabilities of the limit states primarily serve as indicators of safety and reliability [16].

In terms of safety and reliability of steel load bearing structures, the most important variable is the load-carrying capacity (LCC), which can be studied using statistical analysis, e.g. [17], probabilistic analysis, e.g. [18] and sensitivity analysis, e.g. [19–21]. Sensitivity analysis (SA) is a measure of the

^{*} Corresponding author.

E-mail addresses: kala.z@fce.vutbr.cz (Z. Kala), vales.j@fce.vutbr.cz (J. Valeš).

<https://doi.org/10.1016/j.acme.2018.01.009>

1644-9665/© 2018 Politechnika Wroclawska. Published by Elsevier Sp. z o.o. All rights reserved.

importance of input variables [15] and can help researchers understand “how uncertainty in the output of a model (numerical or otherwise) can be apportioned to different sources of uncertainty in the model input” [22].

The technique of SA is as old as that of differential calculus [15]. Various SA approaches are currently being applied in various sub-fields of the civil engineering field [23–25], see also reviews about SA [26–28]. Extensive development of SA and its applications occurred after Sobol's publication of the method based on the decomposition of the output variance [29,30]. Sobol sensitivity analysis (SSA) is referred to as global, because it can quantify the influence of input variables on the model output over the entire range of the distribution and provide the interaction effects between different input variables [31]. Examples of the increasing number of applications of SSA in engineering can be found in [32–37]. Recently there has been a development of new methods of SA based on SSA, for example, the so-called Goal Oriented SA [38] or SA for the measure of the effects of input variables on the structural failure [39].

The aim of the present paper is the SSA [29–31] of the effects of random imperfections on the random LCC of a compressed member with IPN 200 section. LCC is evaluated using the geometric and material non-linear finite element (FE) analysis. Experimental research provides important information on the random variability of initial imperfections of steel members like the yield strength [40–46], geometric deviations in dimensions of the cross-section [41,45], residual stress [47,48], member out-of-straightness [49] and frame out-of-plumb imperfections [50].

In stochastic models, the random realizations of input initial imperfections are simulated using the Monte Carlo method or some form of stratified sampling like Latin Hypercube Sampling (LHS) [51,52]. The realizations of output LCC are then obtained as runs of the non-linear FE model, see e.g. [53,54]. The disadvantage of non-linear FE models is the high computational burden of each run. Therefore, SSA is evaluated in the present article using an approach that approximates the dependence between initial imperfections and LCC using a polynomial metamodel, which is often referred to as a polynomial surrogate model or emulator or approximation model, see e.g. [55–57]. The developed surrogate model replaces the computational expensive full model based on FEM. This approach makes it possible to use a high number of samples of the LHS method and repeat SSA using the step-by-step method for a range of slenderness (lengths) of compressed member IPN 200.

The present study and [54] partially overlap with regard to the non-linear FE model and its random imperfections, however, new results of SSA of LCC of an imperfect compressed member made from steel grades S235 and S355 are presented in the present article. The obtained results are compared with [54]. In order to compare the results of both stability problems, the same IPN 200 section is considered.

It should be noted that the IPN-section is not a representative rolled section for columns, which are more often made from hot-rolled H-sections instead of I-sections. However, the results of SSA pertaining to flexural buckling (FB) can partially be generalized to other narrow flange section members subjected to compression. This is discussed in the conclusion of the present article. In contrast, SSA showed that compressed members (columns) fail due to different combinations

of imperfections than beams in bending. I members subjected to combined compression and bending are not studied in the present paper.

2. Finite element model

The computational model is a column pinned at both ends, which is loaded centrally at one end, see Fig. 1a. The column consists of a double symmetrical rolled European steel cross-section IPN 200. The geometry of the member was slightly simplified and idealized by removing the fillets on the inner sides of the flanges and at the flange-to-web connections in order to maintain regularity of the mesh. Their influence is negligible acc. to [58]. The original and idealized cross-sections are shown in Fig. 1b and c.

The computational model was created using the software Ansys APDL [59]. The SOLID185 element was used for the model. It is a 8-node homogeneous structural solid element that is suitable for 3D modelling of solid structures. It has large deflection and large strain capabilities, plasticity, hyperelasticity, stress stiffening and creep. The enhanced strain formulation was considered. This formulation prevents shear

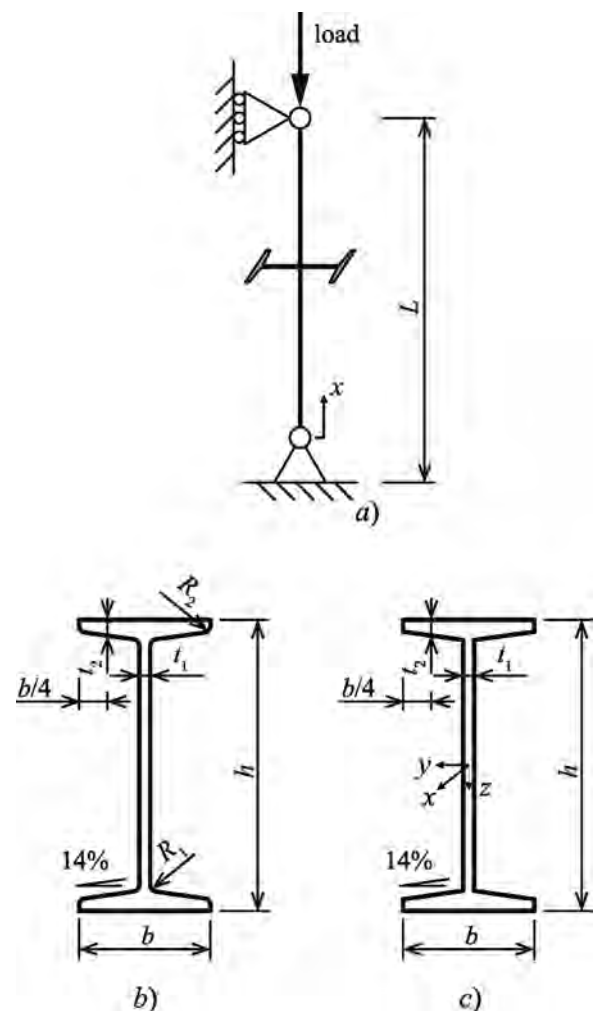


Fig. 1 – (a) Scheme of the compressed member, (b) real cross-section, (c) idealized cross-section.

locking in bending-dominated problems and volumetric locking in nearly incompressible cases. The element introduces nine internal degrees of freedom to handle shear locking, and four internal degrees of freedom to handle volumetric locking. All internal degrees of freedom are introduced automatically at the element level and condensed out during the solution phase of the analysis [59].

2.1. Initial imperfections

Initial geometrical imperfection of the column is considered in the shape of a half-sine wave function in the direction perpendicular to the cross-section axis around which bending due to buckling occurs:

$$y = e_0 \sin\left(\frac{\pi x}{L}\right), \tag{1}$$

where L is the column length and e_0 is the amplitude of initial axial curvature (bow imperfection), which is related to the center of gravity of the cross-section in the middle of the span. This imperfection corresponds to the first eigenmode of beam FB, which is consistent with [60], see also [61].

Initial geometric imperfections are usually introduced as scaled eigenmodes obtained a priori from an elastic buckling analysis, see e.g. [5]. In the present article, the model is created on the basis of Eq. (1), which facilitates modelling using the finite element method. In the case of FB about axis z (FBz), the introduction of bow imperfection can be described as follows: It is possible to derive the coordinates of any point of the beam based on the distance of the center of gravity of the cross-section in the direction of the x -axis from the origin of the coordinate system x_1 , cross-sectional dimensions and the amplitude of initial curvature e_0 , see Fig. 2. The coordinates can then be written in the form of (2):

$$\begin{aligned} x &= x_1 - y_0 \sin\varphi, \\ y &= y_0 \cos\varphi + e_0 \sin\left(\frac{\pi x_1}{L}\right), \\ z &= z_0, \end{aligned} \tag{2}$$

where φ is the angle of rotation of the cross-section about the z -axis given in the form of (3):

$$\varphi = \arctan\left[e_0 \frac{\pi}{L} \cos\left(\frac{\pi x_1}{L}\right)\right], \quad \varphi \in \left(-\arctan\left(e_0 \frac{\pi}{L}\right); \arctan\left(e_0 \frac{\pi}{L}\right)\right). \tag{3}$$

Coordinates y_0 and z_0 are coordinates of an arbitrary point of the cross-section acc. to the scheme in Fig. 3, relative to the local coordinate system of cross-section y^*z^* , where y^*, z^* are principal axes with origin at the center of gravity of the cross-section. The bow imperfection for FB about y -axis (FB y) was introduced analogously.

2.2. FE mesh

Meshing of the cross-section was performed with 10 elements on the flange width, 20 elements on the web height and 2 elements on the web and flange thickness, see Fig. 4. The number of finite elements presents a compromise between the acceptable accuracy and computation time. Two elements on the cross-section thickness may appear to be small, since there is a suspicion that with an 8-node solid element with only three degrees of freedom (dof) in each node, the element might behave poorly in plasticity analysis, because it can only model something corresponding to a constant stress state. Different variants with finer mesh were tested, but had relatively little effect on the accuracy of the LCC [62]. Two values of non-dimensional slenderness, $\bar{\lambda}_z = (0.5; 0.8)$, were considered. In comparison to the mesh applied here, smooth mesh in [62] provides a higher mean value of LCC, but only in

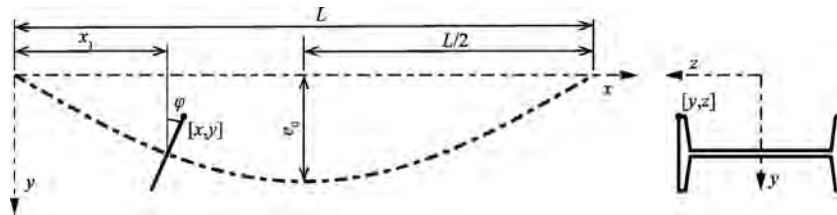


Fig. 2 – Local coordinate system of the cross-section.

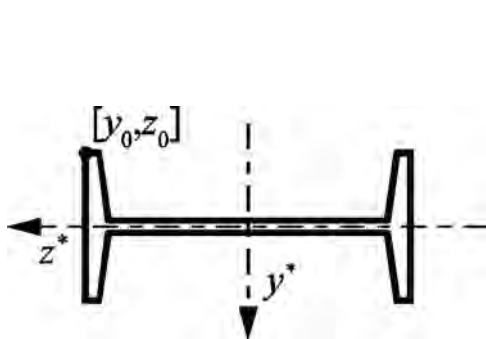


Fig. 3 – Local coordinate system of the cross-section.

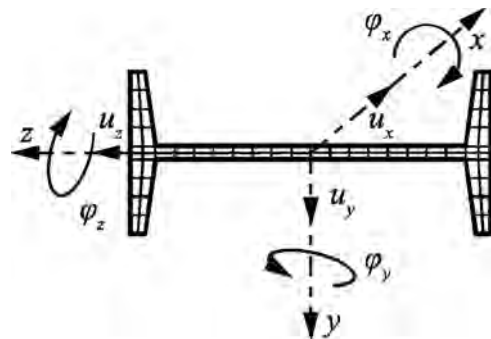


Fig. 4 – Cross-section mesh.

the order of hundreds of percents. The correlation between LCC of a rough and a smooth mesh is almost 1.0 [62]. More elements per thickness led to slightly different stress curves, but had virtually no effect on the resulting resistance. According to [59] the aspect ratio for quadrilaterals should not exceed 20; otherwise, disturbance of analysis results may occur. For this reason, the number of elements per column length was chosen so that the maximum ratio of the longest to the shortest side of the hexahedral of the element was 8. The number of elements per column length is thus linearly dependent on the length of the column. A similar meshing has proven successful in models of beams subjected to bending [54,63]. The FE model with initial imperfection (1) for FBz is shown in Fig. 5.

2.3. Boundary conditions and load

Boundary conditions are introduced for FBz and FBy. For case FBz boundary conditions are introduced on all the nodes in the axes of the web of both end cross-sections, see Fig. 6.

For case FBy translation in the direction of the y-axis ($u_y = 0$) is restricted along the whole length of the member in the axial connections between the web and flanges, see Fig. 7. Furthermore, translation of all nodes lying directly on the y-axis is prevented in the direction of axes x and z ($u_x = u_z = 0$) at one end of the beam ($x = 0$). On the other end ($x = L$) translation is only restricted in the direction of the z-axis, since load is applied here in the direction of the x-axis.

The boundary conditions simulated on both ends, illustrated in Figs. 6 and 7 for $x = 0$ and $x = L$, restrict twist rotation and translations along the principal axes of the section. It should be noted that the warping profile along the flanges in this modelling approach does not comply with the assump-

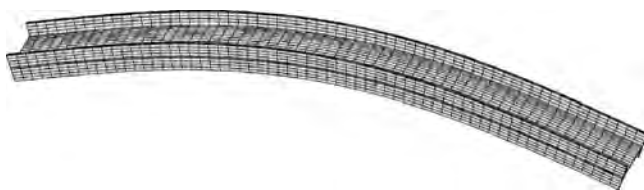


Fig. 5 – FE model in Ansys.

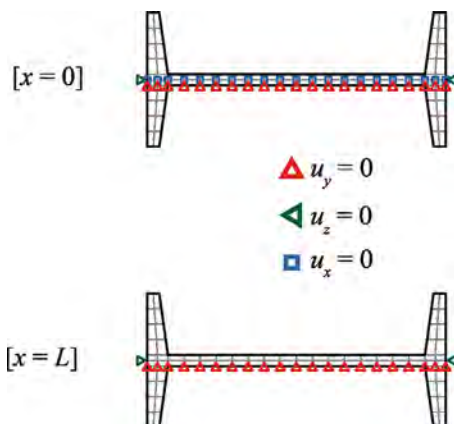


Fig. 6 – Boundary conditions for FBz.

tions used in the beam theory of thin-walled members of open cross-sections.

The load is introduced via a force block at the axial nodes of the web of the end cross-section $x = L$, see Fig. 8. The end sections are modelled in such a way that failure does not occur in the artificial elastic material and the modelled ends of the compressed member are not the limiting factors for the LCC. In order to prevent punching shear on both ends of the compressed member due to stress concentration, the first set of elements behind the end cross-sections are assigned linear elastic material with 100 times higher modulus of elasticity than the adjacent material.

Although such modelling has some differences from the assumptions used in the beam theory of thin-walled open section members, it provides almost identical load-deflection

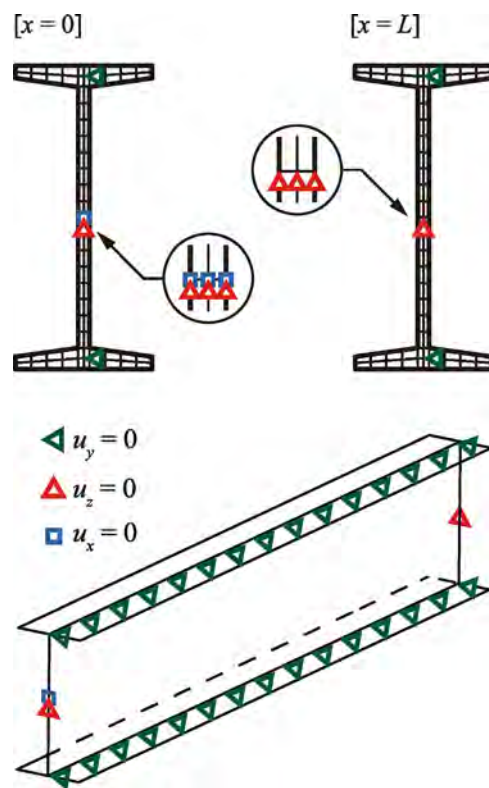


Fig. 7 – Boundary conditions for FBy.

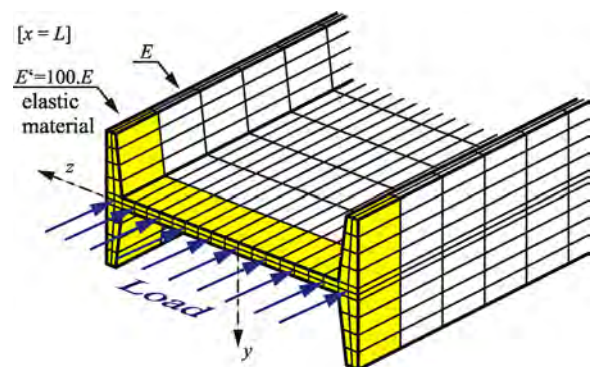


Fig. 8 – Application of force block.

curves in the elastic state. The accuracy of the model was verified by comparing the results of the elastic LCC with the analytical LCC [64], where an almost complete agreement was observed.

2.4. Material model

An elastoplastic material model acc. to ENV 1993-1-5 (Annex C), case b was used. This standard permits the use of a stress-strain diagram with non-zero hardening slope to overcome numerical instability. The value of $E/10000$ was selected for the model, see Fig. 9.

2.5. Residual stress

The buckling capacity is influenced by the residual stress in the member. The temperature dependent production process of rolled sections results in the residual stress distribution in the cross-section and along the length of the section product. These include the rolling temperature, cooling conditions, straightening procedures, and the material properties of the steel [1]. Literature provides many suggestions for the modelling of residual stress in FE-analysis [47,65]. The commonly used residual stress pattern for rolled I sections is the linear stress pattern, see Fig. 10. This pattern was used for the analyses performed in this paper.

The results of numerical simulations found in most references refer the magnitude of residual stresses to either the material yield strength [58,61] or to the nominal stress of f_y , $n = 235$ MPa, see Fig. 10. Experimental research of residual stress in hot-rolled sections of similar shapes produced from different steel grades show that the distribution and magnitude of residual stress are very similar [1,61]. Generally, the residual stress of hot-rolled steel I-beams should not refer to the yield strength without specifying the steel grade and the cross-sectional shape, see the discussion and literature review in [61].

Residual stress distribution of the beam σ_R is introduced into the FE model in the form of equivalent temperate load through initial thermal load step in the manner described in [54,61,63]. The stiffer elastic material of the end sections of the model presented here results in an inconsistency of the final residual stress block at the points of the rolled section ends, see Fig. 11. This inconsistency has no effect on LCC, because the simplified assumption of constant residual stress block along the rolled product length (parent material) is maintained and plasticization starts at $x = L/2$. The rolled section ends are modelled using elastic, one hundred times stiffer blocks in

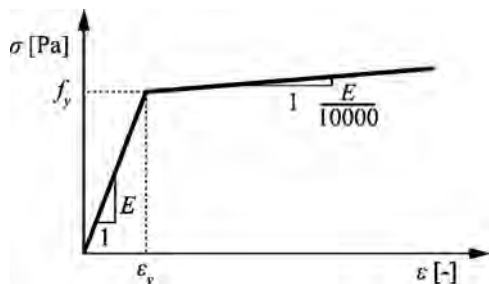


Fig. 9 – Stress-strain diagram.

which failure due to plasticization cannot occur. There is a slight inconsistency of the final stress block in the adjacent touching parent material, however, it is not a factor that would influence the LCC. The correctness of the LCC calculation was verified on compressed column models with artificial end zones (higher modulus of elasticity, higher yield strength) extending up to $L/4$ from the ends of the columns [66].

Temperature change ΔT at a point of the cross-section is given by Eq. (4):

$$\Delta T = -\frac{\sigma_R}{E \cdot \alpha_t} \tag{4}$$

where σ_R is the residual stress at the given point and α_t is the thermal expansion coefficient, considered as $\alpha_t = 1.2E-5$ [K⁻¹]. The distribution of the longitudinal stress σ_x resulting from temperature change ΔT is shown in Fig. 11. $-\sigma_R$ is attained at the end of the flanges and at the centre of the web (blue) while approximately $0.8\sigma_R$ (red) is in the flange-to-web connection.

2.6. Load-carrying capacity

The LCC of the column was evaluated using the geometrical and material non-linear solution with imperfections, including residual stresses. During loading of the column with displacement in the direction of its longitudinal axis, the force reaction R_x is obtained at the other end. The total LCC is defined by the peak of the curve, see Fig. 12.

2.7. Verification of modeling within the elastic range

The modeling described above was verified within the elastic range for $\bar{\lambda}_z = 0.4, 0.5, \dots, 1.6$ [67]. The stochastic comparison of the elastic LCC_E calculated using the FE model described above

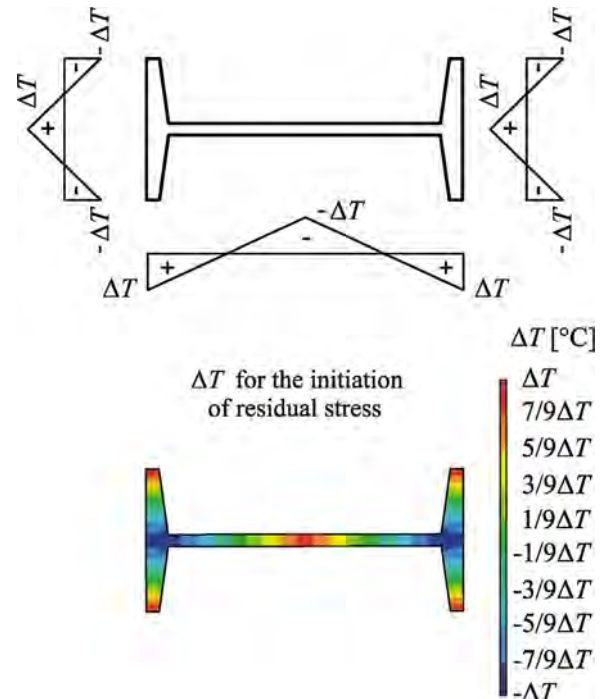


Fig. 10 – Application of linear temperature change ΔT .

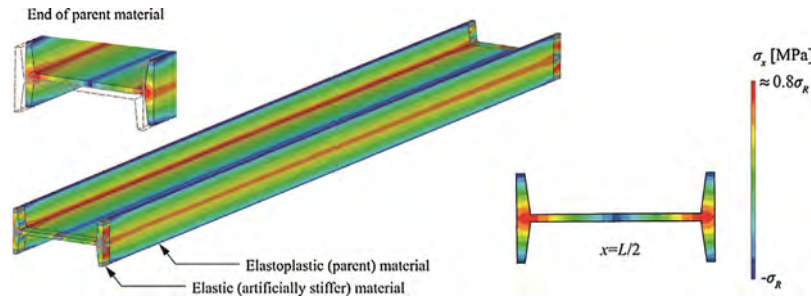


Fig. 11 – Distribution of residual stress initiated by ΔT .

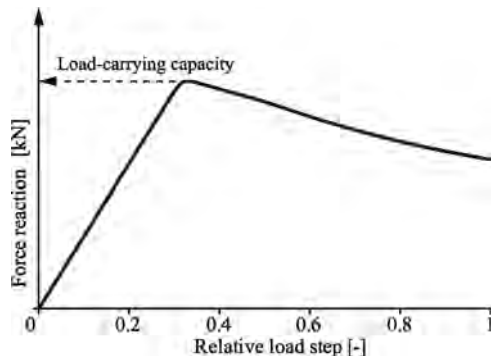


Fig. 12 – Defining the LCC using the force reaction graph.

(but without residual stress and linear stress–strain relationship), and the formula for elastic resistance R based on beam theory published in [64] is provided in [67]. The maximum average relative difference between the R and LCC_E is calculated for $\bar{\lambda}_z = 0.4$ as 1.23%. The correlation between results is almost 1.0 for each slenderness. Such a good match confirms the accuracy of the finite element model within elastic range. Unfortunately, LCC from Fig. 12 was not verified by inelastic analytical solution.

3. Input random imperfections

The columns studied in the present article are produced from carbon steel grades S235 and S355. The yield strength of steel S235 is a random variable whose statistical characteristics were evaluated from 562 samples taken from a third of flanges of hot-rolled European steel members IPE 160 to IPE 220 [41]. The mean value of 297.3 MPa and standard deviation of 16.8 MPa were considered, see Table 1. The probabilistic model

is based on the assumption that the yield stress statistics obtained for IPE sections are also representative for IPN sections. From the technical point of view, the production processes of steel members IPN 200 and IPE 160 to IPE 220 are very similar. The same statistical characteristics of yield strength can be introduced for different types of hot-rolled members of similar dimensions if more accurate data is unavailable [16]. This was applied, for e.g. in [2,68].

It may be noted that the variation coefficient $16.8/297.3 = 0.0565$ is lower than the value of 0.07 listed in probabilistic model [16] in the section Static Properties of Structural Steel-Rolled Sections.

Table 1 lists the statistical characteristics of yield strength of steel S355 taken from [46], where the mean value 393.8 MPa and standard deviation 22 MPa were evaluated from measurements of ten steel sheets. The statistical characteristics [46] are in very good agreement with our measurements from 2001, when the mean value of 394.5 MPa and standard deviation of 19.808 MPa were obtained from the examination of yield strength performed on 243 samples of European hot-rolled steel members U65 to U140 [43]. It may be noted that mean values of 393.8 MPa and 394.5 MPa are almost identical and standard deviation values of 22 MPa and 19.808 MPa differ by approximately 10 percent. The experimentally obtained variation coefficients $22/393.8 = 0.0559$ [46] and $19.808/294.5 = 0.0502$ [43] are lower than the value of 0.07 recommended in [16].

The statistical characteristics of Young's modulus E are taken from [69]. E is considered with mean value of 210 GPa and standard deviation of 10 GPa so as to ensure consistency and comparability with previous studies [34,54,63]. Recent research [70], supported by literature review of 12 sources from the year 1929 to 2002, lists the mean value of 208 GPa and standard deviation of 5.2 GPa obtained from the evaluation of more than 2200 samples. The article [70] draws attention to interesting differences in the statistics of E of steel S235 (S355)

Table 1 – Probabilistic models of input imperfections.

Symbol	Characteristic	Density	Mean	Standard deviation
t_2	Flange thickness	Gauss	11.3 mm	0.518 mm
f_y	Yield strength S235	Gauss	297.3 MPa	16.8 MPa
	Yield strength S355	Gauss	393.8 MPa	22 MPa
E	Modulus of elasticity	Gauss	210 GPa	10 GPa
e_0	Initial imperfection	Gauss	0	$L/1960$
σ_R	Residual stress	Gauss	90 MPa	18 MPa

published in [71], which lists the mean value of 205.5 GPa (209.2 GPa) and standard deviation of 7 GPa (5.4 GPa) from the evaluation of 278 samples of steel S235 (77 samples of steel S355).

The statistical characteristics of flange thickness are considered according to the results of experimental research [45]. The flange tapering (angle of inclination), flange width and other geometric imperfections of the cross-section are considered as deterministic using nominal characteristics. The residual stress at the end of the flanges (see Fig. 11) is considered with the mean value of 90 MPa and variation coefficient 0.2 [47]. The mean value of e_0 is zero and standard deviation $L/1960$ is proportional to the length L so that 95% of observations (LHS runs) of amplitude e_0 lie in the tolerance limits $\pm L/1000$, see e.g. [58,61]. All input random geometric and material imperfections are listed in Table 1.

4. Establishment of a polynomial surrogate model

The relationships between information flowing in and out of the model are often analysed using strategies based on random samples [31]. Unfortunately, the computational burden of the FE model does not permit collection of sufficient LHS runs for real-time SSA evaluation. Therefore, LCC, which is the output of the non-linear FE model, is approximated using a surrogate model (5)

$$LCC \approx Y = \sum_{a=0}^2 \sum_{b=0}^2 \sum_{c=0}^2 \sum_{d=0}^2 \sum_{e=0}^2 c_{\alpha} \cdot X_1^a \cdot X_2^b \cdot X_3^c \cdot X_4^d \cdot X_5^e \quad (5)$$

Polynomial (5) allows the rapid realization of samples without loss of non-linear and interaction effects of input imperfections on the LCC. Polynomial (5) has 243 terms with 243 associated constants c_{α} obtained using the least squares method with 300 + 100 support points, which are stratified using the LHS method [51,52]. The first 300 LHS runs of the FE model are performed for the artificial random variables X_1, X_2, \dots, X_5 in Table 2. The standard deviations in Table 2 are higher than the actual imperfection in Table 1. The reason for introducing higher (artificial) standard deviations is to provide a sufficiently wide domain for approximation (5), which would make it possible to use large numbers of LHS runs in SSA. The other 100 support points of the FE model are realized for (real) probabilistic models of imperfections in Table 1 with settings of the absolute value for each random realization e_0 . The approximation domain of the polynomial (5) is defined by the

minimum and maximum in Table 2 to enable the evaluation of up to 500 thousand LHS runs of random inputs from Table 1.

5. Sobol global sensitivity analysis of LCC

Sobol's method [29,30] is a global sensitivity analysis method, which is based on the principle of variance decomposition, see e.g. [31]. SSA determines the fractional contribution of input factors to the variance of the model output based on a measure of importance [31]. Given a model in the form $Y = f(X_1, X_2, \dots, X_M)$, where Y is a scalar output and X_i are M independent input factors of non-zero variance, the first-order sensitivity index S_i may be defined as [72]:

$$S_i = \frac{V_{X_i}(E_{X_{\sim i}}(Y|X_i))}{V(Y)} \quad (6)$$

where X_i is the i th factor and $X_{\sim i}$ denotes the matrix of all factors but X_i . The variance in the numerator of (6) is the expected reduction in the variance of the model output corresponding to the fixing of X_i . The variance $V(Y)$ in the denominator of (6) is the total (unconditioned) variance. The second-order sensitivity index S_{ij} can be written as:

$$S_{ij} = \frac{V_{X_i X_j}(E_{X_{\sim ij}}(Y|X_i, X_j))}{V(Y)} \quad (7)$$

where X_j is the j th factor and $X_{\sim ij}$ denotes the matrix of all factors but X_i, X_j ; and so on for higher order indices. The total number of Sobol indices is $2^M - 1$. The sum of all Sobol indices is equal to one.

$$\sum_i S_i + \sum_i \sum_{j>i} S_{ij} + \sum_i \sum_{j>i} \sum_{k>j} S_{ijk} + \dots + S_{123\dots M} = 1 \quad (8)$$

Relations for the second and higher order indices hold if the input factors are independent, which is the setting adopted throughout the present work. The method for numerical calculation (6) based on the LHS method was practically described e.g. in [73].

In the study presented here, SSA is performed using the polynomial approximation of the model output Y (5). The sensitivity indices are evaluated using the LHS approach from the pdfs in Table 1. Computation of V_{X_i} has the computational burden of ten thousand samples of $E_{X_{\sim i}}(Y|X_i)$, where one sample of $E_{X_{\sim i}}(Y|X_i)$ is computed using ten thousand independent runs. The total computational cost for the evaluation of the numerator (6) is $10,000^2$ runs. The denominator in (6) is

Table 2 – Artificial random variables for approximation.

Symbol	Characteristic	Density	Minimum	Maximum
X_1	Flange thickness	Rectangular	8.83 mm	13.77 mm
X_2	Yield strength S235	Rectangular	217.43 MPa	377.17 MPa
	Yield strength S355	Rectangular	289.21 MPa	498.39 MPa
X_3	Modulus of elasticity	Rectangular	162.46 GPa	257.54 GPa
X_4	Initial imperfection	Rectangular	0	4.76 L/1960
X_5	Residual stress	Rectangular	0 MPa	180 MPa

Table 3 – Member length L vs. non-dimensional slenderness.

Buckling	Steel	Function	Domain
About axis z	S235	$L \approx 1.78 \cdot \lambda_2^A$	$\lambda_2^A \in (0, \infty)$
About axis z	S355	$L \approx 1.44 \cdot \lambda_2^A$	$\lambda_2^A \in (0, \infty)$
About axis y	S235	$L \approx 7.51 \cdot \lambda_2^A$	$\lambda_2^A \in (0, \infty)$
About axis y	S355	$L \approx 6.11 \cdot \lambda_2^A$	$\lambda_2^A \in (0, \infty)$
LTB	S235	$L \approx 2.04 \cdot \lambda_{LT}^A - 0.4 \cdot \lambda_{LT}^B + 1.63 \cdot \lambda_{LT}^C - 0.3 \cdot \lambda_{LT}^D$	$\lambda_{LT}^A \in (0, 2)$

Where unit of L is [m] and units of $\lambda_2^A, \lambda_2^B, \lambda_{LT}^A$ are non-dimensional.

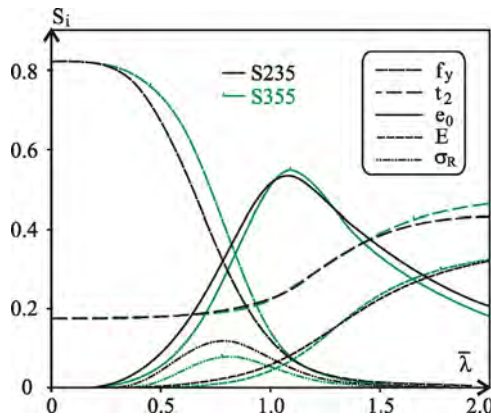


Fig. 13 – SSA of LCC – FBz.

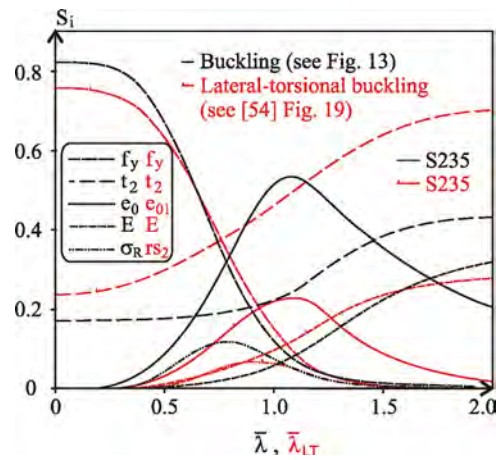


Fig. 15 – S_i from FBz vs. S_i from LTB [54].

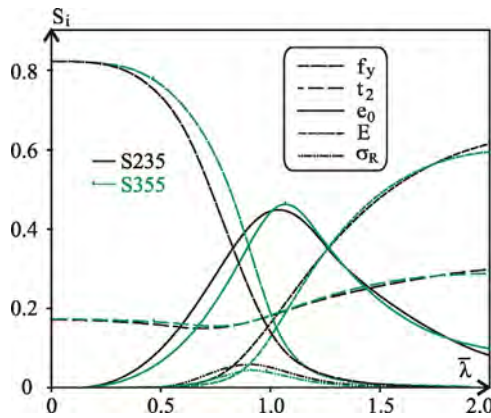


Fig. 14 – SSA of LCC – FBy.

evaluated from 500 thousand LHS runs, which is a relatively low computational burden. The mentioned number of runs is used for the evaluation of each of the $2^5 - 1 = 31$ sensitivity indices.

6. Sensitivity analysis results

Non-dimensional slenderness $\bar{\lambda}_z$ and $\bar{\lambda}_y$ defined in [74] were considered as deterministic parameters, which were changed using the step-by-step method with the step of 0.01. The values of L for the IPN 200 member can be approximately calculated using the relations in Table 3.

There are two main SSA result groups, which are very similar in buckling tasks. The first group associates indices S_i of FBz, see Fig. 13. The second group associates S_i of FBy, see Fig. 14. In each group, SSA results for two steel grades S235 and S355 are similar with the exception of the influence of residual stress, which is more significant in steel S235, and the influence of yield strength, which is more significant in steel S355.

Greater differences are evident from the comparison of Figs. 13 and 14. There is higher sensitivity to e_0, σ_R, t_2 and on the contrary, lower sensitivity to E and f_y in Fig. 13. Indices S_i are the same if $\bar{\lambda} = 0$. It is interesting that (i) the green curve S_{f_y} in Fig. 13 (S355, FBz) is the same as (ii) the black curve S_{f_y} in Fig. 14 (S235, FBy). The overlap S_{f_y} (i) and (ii) does not mean the same for S_i of the other imperfections, where for $\bar{\lambda} < 0.9$ we observe higher values of S_{t_2} and S_{σ_R} and lower values of S_{e_0} for S355 in Fig. 13 (green curve) in comparison with S_{t_2}, S_{σ_R} and S_{e_0} shown for S235 in Fig. 14 (black curve).

Fig. 15 shows the comparison of indices S_i from Fig. 13 with S_i determined for hot-rolled steel beam IPN 200 subjected to lateral-torsional buckling (LTB) due to bending moment about the major principal axis, see [54] Fig. 19. The present study and [54] are based on a similar FE model and use the same pdfs of $t_2, f_y, E, e_0, \sigma_R$. However, different loads and different stability phenomena are considered in the evaluation of the LCC. It is apparent from Fig. 15 that the LCC of the compressed column is more than twice more sensitive to the initial imperfection e_0 , which is an unexpectedly big difference. For the increasing part of the curve S_{e_0} it holds that the ratio of the black S_{e_0} (FBz) to red S_{e_0} (LTB) is constant at approximately 2.34, i.e. the

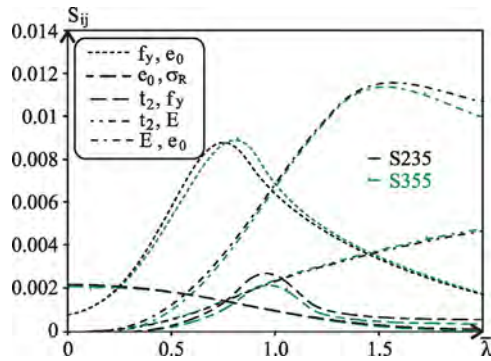


Fig. 16 – SSA of LCC – FBz.

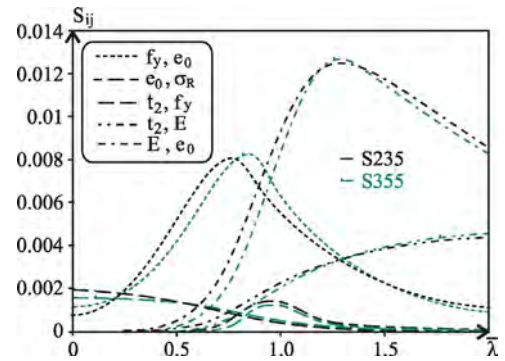


Fig. 17 – SSA of LCC – FBy.

increasing part of the curve (approximately for $\bar{\lambda} < 1.1$) is similar in shape, but has a different scale. For $\bar{\lambda} < 1.1$ LCC of the compressed column is more sensitive to the variability of residual stress, but for $\bar{\lambda} > 1.1$ S_{σ_R} are practically identical. LCC of a member under bending is more sensitive to the flange thickness t_2 . The effects of f_y , E are approximately the same in both cases. Similar observations can be made from the comparison of Fig. 15 (LTB) and Fig. 14 (S235), with the difference that S_{σ_R} are approximately equal and approximately double the influence of E is apparent from Fig. 14.

Higher-order interactions are relatively small in comparison with, for e.g., SSA results of frame systems [73]. However, they supplement the information on the overall effect of imperfections on LCC. Figs. 16 and 17 show the values of the largest second-order sensitivity indices, the remaining higher-order sensitivity indices are lower and are not plotted. The decisive second-order interaction is from the pairs E , e_0 and f_y , e_0 . In all of the cases of slenderness solved here, f_y is involved in the higher-order interactions. This is the difference in comparison with SSA of LTB [54], where interaction between f_y and other imperfections did not occur for $\bar{\lambda}_{LT} > 2.0$.

Figs. 13, 14, 16 and 17 show that the results of SSA obtained for S235 and S355 are very similar, therefore $\bar{\lambda}$ is a good common platform for the analysis of the ultimate limit state of compressed columns.

In the presented tasks, SSA was performed for compressed columns with $\bar{\lambda} \leq 2$, higher slenderness was not examined. The reason is that very slender columns are seldom designed in building practice and SSA would require much more computation time than in the case of columns with intermediate slenderness. However, the results of SSA showed that imperfections e_0 and f_y may also be involved in higher-order interactions for $\bar{\lambda} > 2$. From this perspective, it may be interesting to examine the interactions between plasticity and instability effects for higher slenderness values. The question is: From what value of $\bar{\lambda}$ will higher-order interactions between f_y and other imperfections disappear and the calculation of LCC become totally insensitive to plastic yielding? At the same time, it may be interesting to investigate whether there exists such a value of $\bar{\lambda}$, which when exceeded $S_{e_0} = 0$ and all higher-order sensitivity indices involved in interactions with e_0 will be equal to zero. Answering these questions may present a new link between the classical solution based on Euler's critical force and the response of a real imperfect column.

For elastic resistance determined from analytical statistical models [34,64], it is typical that the sensitivity to e_0 is maximum for $\bar{\lambda} \approx \bar{\lambda}_{LT} \approx 0.9$. In contrast, the FE models presented here and in [54] have shown that the maximum sensitivity to e_0 occurs for $\bar{\lambda} \approx \bar{\lambda}_{LT} \approx 1.1$, see Fig. 13 (presented here), Fig. 14 (presented here) and Fig. 19 (presented in [54]). FE modelling in comparison to conventional analytical approaches is capable of analysing the effects of imperfection e_0 and residual stress separately. Maximum sensitivity to the residual stress occurs for $\bar{\lambda}_{LT} \approx 0.9$ in the case of LTB [54], which also applies to the results presented here in Fig. 14 (FBy). However, this does not apply to the results in Fig. 13 (FBz), which show that the maximum sensitivity to residual stress occurs for $\bar{\lambda} \approx 0.8$. However, from a technical point of view, it is a relatively small difference.

7. Conclusion

SSA of LCC of columns of steel S235 and S355 yielded similar results in the case of buckling about one axis y or z . This conclusion applies to both first order sensitivity indices and second order sensitivity indices. It confirms the validity of the Eurocode 3 concept in which non-dimensional slenderness $\bar{\lambda}$ is introduced as a common platform for the determination of the design buckling resistance.

The following conclusions can be drawn from the comparison of SSA of LCC pertinent to FBz with FBy:

- FBz is more sensitive than FBy to imperfection e_0 , flange thickness t_2 , residual stress σ_R , see Figs. 13 and 14.
- FBy is more sensitive than FBz to Young's modulus E and yield strength f_y , see Figs. 13 and 14.
- FBz has maximum S_{σ_R} when $\bar{\lambda} = 0.8$ while FBy has maximum S_{σ_R} when $\bar{\lambda} = 0.9$, see Figs. 13 and 14.
- Both FBz, FBy have maximum S_{e_0} when $\bar{\lambda} \approx 1.1$, see Figs. 13 and 14.
- FBz has the same curve S_{f_y} for S355 as FBy S_{f_y} for S235, see Figs. 13 and 14.
- Both FBz, FBy have the same S_i when $\bar{\lambda} = 0$, see Figs. 13 and 14.
- Both FBz, FBy have identified dominant interaction of pairs E , e_0 and f_y , e_0 between all the other pairs, see Figs. 16 and 17.
- Eurocode introduces a more conservative buckling curve (higher imperfection factor α) for FBz than for FBy. Taking into account the results of SSA it can be concluded that

higher sensitivity to e_0 , t_2 , σ_R found in FBz is taken into account in Eurocode 3 by a higher value of imperfection factor α . It can be noted that Eurocode 3 applies the imperfection factor α only to the shape of the cross-section and the axis of bending. The differences between FBz and FBy identified here indicate other relevant circumstances that may affect Eurocode 3 design criteria of reliability.

From the comparison of SSA of LCC pertinent to FBz with LTB [54] we can observe two important differences:

- FBz is more than twice more sensitive to imperfection e_0 than LTB, see Fig. 15.
- LTB is more sensitive to t_2 than FBz, see Fig. 15.

The maximum sensitivity to e_0 in elastoplastic FE models occurs for higher non-dimensional slenderness ($\bar{\lambda} \approx \bar{\lambda}_{LT} \approx 1.1$) than in elastic analytical models ($\bar{\lambda} \approx \bar{\lambda}_{LT} \approx 0.9$). The elastic resistance of analytical models [34,64] is most sensitive to e_0 for non-dimensional slenderness 0.9, which is also the value for which LCC of the FE model [54] is most sensitive to the residual stress. The SSA results presented here corroborate the conclusions of [54] on the possibilities of substituting the effect of residual stress with the equivalent initial geometrical imperfection, which is often introduced for design purposes in practice, see e.g. [75].

The maximum value S_{e0} for FBz is twice higher than the maximum value S_{e0} for LTB, see Fig. 15. The reliability of members with intermediate and higher slenderness subjected to bending can be economically ensured, in particular by reducing the random variability of t_2 in production. On the other hand, it would be most effective in the case of columns under compression to reduce the random variability of e_0 , which is technically and economically more demanding.

The yield strength is the dominant variable for steel members with low slenderness. As was discussed in the article, the variation coefficients of the yield strength of the flanges of hot-rolled members of steel S235 and S355 obtained from experimental research [41,43] are lower than the conservative value of 0.07 recommended in [16].

The SSA presented here was applied to a specific member with cross-section IPN 200. Although the IPN 200 section is not a representative rolled section, the SSA results have clearly shown the effects of initial imperfections of such a member, whose principal second moments of area are relatively different. According to our recent numerical experience, the findings and conclusions presented here can be approximately generalized and applied to other IPN and IPE hot-rolled (Class 1) section columns, whose cross-sections are close to IPN 200. Similarities in SSA results were also found for FBy of H section compression members with intermediate slenderness. However, there is a greater influence of σ_R and a smaller influence of e_0 in the case of FBz of H section members with intermediate slenderness. This conclusion, however, needs to be verified and supplemented by further studies.

Ethical statement

Authors state that the research was conducted according to ethical standards.

Acknowledgements

This result was prepared with the financial support of the projects GAČR 17-02862S and LO1408 “AdMAs UP”.

REFERENCES

- [1] R.D. Ziemian, *Guide to Stability Design Criteria for Metal Structures*, John Wiley & Sons, New Jersey, 2010.
- [2] J. Szalai, F. Papp, On the probabilistic evaluation of the stability resistance of steel columns and beams, *J. Construct. Steel Res.* 65 (2009) 569–577.
- [3] V. Papadopoulos, G. Soimiris, M. Papadrakakis, Buckling analysis of I-section portal frames with stochastic imperfections, *Eng. Struct.* 47 (2013) 54–66.
- [4] D. Schillinger, *Stochastic FEM Based Stability Analysis of I-Sections With Random Imperfections*, (Diploma thesis), Stuttgart University, 2008.
- [5] S. Shayan, K. Rasmussen, H. Zhang, *On the Modelling of Initial Geometric Imperfections and Residual Stress of Steel Frames*, The University of Sydney, 2012.
- [6] G. Sedlacek, H. Stangenberg, Design philosophy of Eurocodes – background information, *J. Construct. Steel Res.* 54 (1) (2000) 173–190.
- [7] G. Sedlacek, Ch. Müller, The European standard family and its basis, *J. Construct. Steel Res.* 62 (11) (2006) 1047–1059.
- [8] ISO 2394:2015, *General Principles on Reliability for Structures. The International Standard*, International Organization for Standardization, Geneva, 1998.
- [9] EN 1990, *Eurocode-Basic of Structural Design*, CEN, Brussels, 2002.
- [10] S.K. Dugal, *Limit State Design of Steel Structures*, Tata McGraw-Hill Education India, India, 2014.
- [11] K. Lee, J.S. Davidson, J. Choi, Y. Kang, Ultimate strength of horizontally curved steel I-girders with equal end moments, *Eng. Struct.* 153 (2017) 17–31.
- [12] J. Chalmovský, J. Štefaňák, L. Miča, Z. Kala, Š. Skuodis, A. Norkus, D. Žilionienė, Statistical-numerical analysis for pullout tests of ground anchors, *Baltic J. Road Bridge Eng.* 12 (3) (2017) 145–153.
- [13] E.K. Zavadskas, Z. Turskis, S. Kildienė, State of art surveys of overviews on MCDM/MADM methods, *Technol. Econ. Dev. Econ.* 20 (2014) 165–179.
- [14] J. Antucheviciene, Z. Kala, M. Marzouk, E.R. Vaidogas, Solving civil engineering problems by means of fuzzy and stochastic MCDM methods: current state and future research, *Math. Probl. Eng.* 2015 (2015) 1–16, Article ID 362579.
- [15] O. Ditlevsen, H.O. Madsen, *Structural Reliability Methods*, John Wiley & Sons, Chichester, 1996.
- [16] Code. Model, Joint Committee of Structural Safety, JCSS, 2001 Available from: <http://www.jcss.ethz.ch>.
- [17] C. Rebelo, N. Lopes, L. Simões da Silva, D. Nethercot, PMM Vila Real, Statistical evaluation of the lateral-torsional buckling resistance of steel I-beams. Part 1: Variability of the Eurocode 3 resistance model, *J. Construct. Steel Res.* 65 (2009) 818–831.
- [18] Z. Kala, Reliability analysis of the lateral torsional buckling resistance and the ultimate limit state of steel beams with random imperfections, *J. Civil Eng. Manage.* 21 (7) (2015) 902–911.
- [19] D. Schillinger, V. Papadopoulos, M. Bischoff, M. Papadrakakis, Buckling analysis of imperfect I-section beam-columns with stochastic shell finite elements, *Comput. Mech.* 46 (3) (2010) 495–510.

- [20] S. Moradi, M.S. Alamb, A.S. Milani, Cyclic response sensitivity of post-tensioned steel connections using sequential fractional factorial design, *J. Construct. Steel Res.* 112 (2015) 155–166.
- [21] M. Kotelko, P. Lis, M. Macdonald, Load capacity probabilistic sensitivity analysis of thin-walled beams, *Thin-Walled Struct.* 115 (2017) 142–153.
- [22] A. Saltelli, P. Annoni, I. Azzini, F. Campolongo, M. Ratto, S. Tarantola, Variance based sensitivity analysis of model output, *Des. Estim. Total Sensit. Index* 181 (2) (2010) 256–270.
- [23] R. Sousa, J. Guedes, H. Sousa, Characterization of the uniaxial compression behaviour of unreinforced masonry—sensitivity analysis based on a numerical and experimental approach, *Arch. Civil Mech. Eng.* 15 (2015) 532–547.
- [24] J. Ferreiro-Cabello, E. Fraile-Garcia, E. Martinez-Camara, M. Perez-de-la-Parte, Sensitivity analysis of Life Cycle Assessment to select reinforced concrete structures with one-way slabs, *Eng. Struct.* 132 (2017) 586–596.
- [25] O. Mirza, S.K. Shill, F. Mashiri, D. Schroot, Behaviour of retrofitted steel structures using cost effective retrofitting techniques, *J. Construct. Steel Res.* 131 (2017) 38–50.
- [26] E. Borgonovo, E. Plischke, Sensitivity analysis: a review of recent advances, *Eur. J. Oper. Res.* 248 (3) (2016) 869–887.
- [27] P. Wei, Z. Lu, J. Song, Variable importance analysis: a comprehensive review, *Reliab. Eng. Syst. Saf.* 142 (2015) 399–432.
- [28] F. Ferretti, A. Saltelli, S. Tarantola, Trends in sensitivity analysis practice in the last decade, *Sci. Total Environ.* 568 (2016) 666–670.
- [29] I.M. Sobol', Sensitivity estimates for nonlinear mathematical models, *Math. Model. Comput. Exp.* 1 (4) (1993) 407–414 (Translated from Russian. Sobol', I.M. Sensitivity estimates for nonlinear mathematical models. *Matematicheskoe Modelirovanie* 2 (1) (1990) 112–118.).
- [30] I.M. Sobol', Global sensitivity indices for nonlinear mathematical models and their Monte Carlo estimates, *Math. Comput. Simul.* 55 (1–3) (2001) 271–280.
- [31] A. Saltelli, K. Chan, E.M. Scott, *Sensitivity Analysis*, Wiley Series in Probability and Statistics, John Wiley & Sons, New York, 2004.
- [32] E. Patelli, H.J. Pradlwarter, G.I. Schuëller, Global sensitivity of structural variability by random sampling, *Comput. Phys. Commun.* 181 (12) (2010) 2072–2081.
- [33] D. Mukherjee, B.N. Rao, A. Meher Prasad, Global sensitivity analysis of unreinforced masonry structure using high dimensional model representation, *Eng. Struct.* 33 (4) (2011) 1316–1325.
- [34] Z. Kala, Sensitivity and reliability analyses of lateral-torsional buckling resistance of steel beams, *Arch. Civil Mech. Eng.* 15 (2015) 1098–1107.
- [35] Z. Hu, S. Mahadevan, Uncertainty quantification in prediction of material properties during additive manufacturing, *Scr. Mater.* 135 (2017) 135–140.
- [36] A.H. Arshian, G. Morgenthal, Probabilistic assessment of the ultimate load-bearing capacity in laterally restrained two-way reinforced concrete slabs, *Eng. Struct.* 150 (2017) 52–63.
- [37] K. Cheng, Z. Lu, Adaptive sparse polynomial chaos expansions for global sensitivity analysis based on support vector regression, *Comput. Struct.* 194 (2018) 86–96.
- [38] J. Fort, T. Klein, N. Rachdi, New sensitivity analysis subordinated to a contrast, *Commun. Stat.-Theory Methods* 45 (15) (2016) 4349–4364.
- [39] S. Xiao, Z. Lu, Structural reliability sensitivity analysis based on classification of model output, *Aerospace Sci. Technol.* 71 (2017) 52–61.
- [40] F.M. Bartlett, R.J. Dexter, M.D. Graeser, J.J. Jelinek, B.J. Schmidt, T.V. Galambos, Updating standard shape material properties database for design and reliability, *Eng. J.* 40 (1) (2003) 2–14.
- [41] J. Melcher, Z. Kala, M. Holický, M. Fajkus, L. Rozlívka, Design characteristics of structural steels based on statistical analysis of metallurgical products, *J. Construct. Steel Res.* 60 (3–5) (2004) 795–808.
- [42] A. Strauss, Z. Kala, K. Bergmeister, S. Hoffmann, D. Novák, The object of this contribution is the comparison of the statistical characteristics of yield strength, ultimate strength and ductility of Austrian and Czech steels [Technologische eigenschaften von stählen im europäischen vergleich], *Stahlbau* 75 (1) (2006) 55–60.
- [43] J. Melcher, Z. Kala, M. Karmazínová, M. Fajkus, M. Holický, L. Rozlívka, L. Puklický, Statistical evaluation of material characteristics and their influence on design strength of structural steel of S355, *Proc. of Int. Conf. Eurosteel 2008* (2008) 809–814.
- [44] L. Simões da Silva, C. Rebelo, D. Nethercot, L. Marques, R. Simões, P.M.M. Vila Real, Statistical evaluation of the lateral-torsional buckling resistance of steel I-beams. Part 2: Variability of steel properties, *J. Construct. Steel Res.* 65 (2009) 832–849.
- [45] Z. Kala, J. Melcher, L. Puklický, Material and geometrical characteristics of structural steels based on statistical analysis of metallurgical products, *J. Civil Eng. Manage.* 15 (3) (2009) 299–307.
- [46] A. Sadowski, J.M. Rotter, T. Reinke, T. Ummenhofer, Statistical analysis of the material properties of selected structural carbon steels, *Struct. Saf.* 53 (2015) 26–35.
- [47] S. Shayan, K.J.R. Rasmussen, H. Zhang, Probabilistic modelling of residual stress in advanced analysis of steel structures, *J. Construct. Steel Res.* 101 (2014) 407–414.
- [48] H. Pasternak, G. Kubieniec, Implementation of longitudinal welding stresses into structural calculation of steel structures, *J. Civil Eng. Manage.* 22 (1) (2016) 47–55.
- [49] M. Zeinoddini, B.W. Schafer, Simulation of geometric imperfections in cold-formed steel members using spectral representation approach, *Thin-Walled Struct.* 60 (2012) 105–117.
- [50] S. Shayan, K. Rasmussen, H. Zhang, On the modelling of initial geometric imperfections of steel frames in advanced analysis, *J. Construct. Steel Res.* 98 (2014) 167–177.
- [51] M.D. McKey, W.J. Conover, R.J. Beckman, A comparison of the three methods of selecting values of input variables in the analysis of output from a computer code, *Technometrics* 21 (2) (1979) 239–245.
- [52] R.C. Iman, W.J. Conover, Small sample sensitivity analysis techniques for computer models with an application to risk assessment, *Commun. Stat. – Theory Methods* 9 (17) (1980) 1749–1842.
- [53] Z. Kala, J. Valeš, J. Jönsson, Random fields of initial out of straightness leading to column buckling, *J. Civil Eng. Manage.* 23 (7) (2017) 902–913.
- [54] Z. Kala, J. Valeš, Global sensitivity analysis of lateral-torsional buckling resistance based on finite element simulations, *Eng. Struct.* 134 (2017) 37–47.
- [55] A.I.J. Forrester, A.J. Keane, Recent advances in surrogate-based optimization, *Prog. Aerospace Sci.* 45 (2009) 50–79.
- [56] J. Wu, Z. Luo, J. Zheng, C. Jiang, Incremental modeling of a new high-order polynomial surrogate model, *Appl. Math. Model.* 40 (2016) 4681–4699.
- [57] W. Liu, X. Wu, L. Zhang, J. Zheng, J. Teng, Global sensitivity analysis of tunnel-induced building movements by a precise metamodel, *J. Comput. Civil Eng.* 31 (5) (2017) 1–16. , [http://dx.doi.org/10.1061/\(ASCE\)CP.1943-5487.0000681](http://dx.doi.org/10.1061/(ASCE)CP.1943-5487.0000681), Article number 04017037.
- [58] P. Kaim, *Spatial buckling behaviour of steel members under bending and axial compression*, (Ph.D. thesis), Technischen Universität Graz, 2004.
- [59] ANSYS Theory Release 15.1, ANSYS Inc., 2014.
- [60] ENV 1993-1-5:2006, Eurocode 3: Design of Steel Structures – Part 1.5: Plated structural elements, CEN – European committee for Standardization, Brussels (Belgium), 2006.

- [61] J. Jönsson, T.C. Stan, European column buckling curves and finite element modelling, *J. Construct. Steel Res.* 128 (2017) 136–151.
- [62] J. Valeš, Z. Kala, Mesh convergence study of solid FE model for buckling analysis, *Proc. of 15th Int. Conf. ICNAAM 2017* (2017) 1–4.
- [63] Z. Kala, J. Valeš, Stochastic assessment and lateral–torsional buckling design of I-beams, *J. Construct. Steel Res.* 139 (2017) 110–122.
- [64] Z. Kala, Sensitivity assessment of steel members under compression, *Eng. Struct.* 31 (6) (2009) 1344–1348.
- [65] M. Abambres, W.M. Quach, Residual stresses in steel members: a review of available analytical expressions, *Int. J. Struct. Integr.* 7 (1) (2016) 70–94.
- [66] J. Valeš, Sensitivity analysis of static resistance of slender beam under bending, in: *AIP Conf. Proc.*, vol. 1738, 2016, <http://dx.doi.org/10.1063/1.4952169>, 380008-1–380008-4.
- [67] J. Valeš, Z. Kala, Weak axis buckling – elastic resistance of a column, in: *CD Proc. of 23rd Int. Conf. on Engineering Mechanics*, 2017, 1014–1017, Accession Number: WOS: 000411657600243.
- [68] A.K. Kazantzi, T.D. Righiniotis, M.K. Chryssanthopoulos, The effect of joint ductility on the seismic fragility of a regular moment resisting steel frame designed to EC8 provisions, *J. Construct. Steel Res.* 64 (2008) 987–996.
- [69] G.C. Soares, Uncertainty modelling in plate buckling, *Struct. Saf.* 5 (1) (1988) 17–34.
- [70] Z. Mendera, M. Suchodola, Partial safety factors in designing of steel structures according to Eurocodes, *Inżynieria i Budownictwo* 12 (2013) 667–672 (in Polish).
- [71] M. Rhode, *Zur Qualitätssicherung Mechanische Eigenschaften von Baustahl*, (PhD thesis), Technischen Universität Braunschweig, 1987.
- [72] A. Saltelli, P. Annoni, How to avoid a perfunctory sensitivity analysis, *Environ. Model. Softw.* 25 (2010) 1508–1517.
- [73] Z. Kala, Global sensitivity analysis in stability problems of steel frame structures, *J. Civil Eng. Manage.* 22 (3) (2016) 417–424.
- [74] ENV 1993-1-1:1992, Eurocode 3: Design of Steel Structures – Part 1.1: General Rules and Rules for Buildings, CEN – European committee for Standardization, Brussels (Belgium), 1992.
- [75] T. Tankova, L. Marques, A. Andrade, L. Simões da Silva, A consistent methodology for the out-of-plane buckling resistance of prismatic steel beam-columns, *J. Construct. Steel Res.* 128 (2017) 839–852.